mathematics

MDPI

Article

A Novel Approach for Improving Reverse Osmosis Model Accuracy: Numerical Optimization for Water Purification Systems

Samad Noeiaghdam [1,*] and Sanda Micula [2]

[1] Institute of Mathematics, Henan Academy of Sciences, Zhengzhou 450046, China
[2] Department of Mathematics and Computer Science, Babeş-Bolyai University, 400084 Cluj-Napoca, Romania; sanda.micula@ubbcluj.ro
* Correspondence: snoei@hnas.ac.cn

Abstract: The primary objective of this study is to present a new technique and library designed to validate the outcomes of numerical methods used for addressing various issues. This paper specifically examines the reverse osmosis (RO) model, a well-known water purification system. A crucial aspect of this problem involves solving an integral that is part of the overall solution. This integral is handled using one of the quadrature integration methods, with a focus on Romberg integration in this study. To manage the number of iterations, as well as to ensure accuracy and minimize errors, we employ the CESTAC method (Controle et Estimation Stochastique des Arrondis de Calculs) alongside the CADNA (Control of Accuracy and Debugging for Numerical Applications) library. By implementing this approach, we aim to achieve not only optimal results, but also the best method step and minimal error, and we aim to address numerical instabilities. The results show that only 16 iterations of the Romberg integration rule will be enough to find the approximate solutions.To demonstrate the efficacy and precision of our proposed method, we conducted two comprehensive comparative studies with the Sinc integration. The first study compares the optimal iteration count, optimal approximation, and optimal error between the single and double exponential decay methods and the Romberg integration technique. The second study evaluates the number of iterations required for convergence within various predefined tolerance values. The findings from both studies consistently indicate that our method outperforms the Sinc integration in terms of computational efficiency. Additionally, these comparative analyses highlight the potential of our approach as a reliable and effective tool for numerical integration.

Keywords: reverse osmosis system; Romberg integration; CESTAC method; CADNA library

MSC: 65D30

check for updates

Academic Editors: Maria Filomena Teodoro and Marina A. P. Andrade

Received: 12 January 2025
Revised: 24 January 2025
Accepted: 26 January 2025
Published: 30 January 2025

Citation: Noeiaghdam, S.; Micula, S. A Novel Approach for Improving Reverse Osmosis Model Accuracy: Numerical Optimization for Water Purification Systems. *Mathematics* **2025**, *13*, 459. https://doi.org/10.3390/math13030459

Correction Statement: This article has been republished with a minor change. The change does not affect the scientific content of the article and further details are available within the backmatter of the website version of this article.

Copyright: © 2025 by the authors. Licensee MDPI, Basel, Switzerland. This article is an open access article distributed under the terms and conditions of the Creative Commons Attribution (CC BY) license (https://creativecommons.org/licenses/by/4.0/).

1. Introduction

There is no denying the importance of mathematical models in our lives. We may represent and evaluate a wide range of issues using linear and nonlinear models [1]. The RO model, which can create drinking water based on a semi-permeable membrane that eliminates undesirable molecules and bigger particles like ions from water, is one of the most significant and useful procedures in water treatment [2]. A significant body of research has been dedicated to the modeling, optimization, and application of RO in water treatment and desalination. For instance, the study in [3] delved into the modeling and optimization of reverse salt, while ref. [4] explored the optimization of reverse osmosis desalination from

brackish waters. Furthermore, the solution-diffusion model for water transport in reverse osmosis was elucidated in [5], providing valuable insights into the underlying mechanisms of the process.

In recent years, several researchers have made notable contributions to the field of RO. Y. Zhai et al. [6] investigated the feasibility of a one-step RO process for drinking water purification, highlighting its potential as an efficient and effective method. Meanwhile, B. Zhang et al. [7] examined the issue of membrane fouling in reverse osmosis filters, a critical concern in maintaining the performance and longevity of RO systems. S. Jamil et al. [8] explored the application of pressure-assisted forward osmosis for water purification, demonstrating its promise as an alternative approach.

Additional studies have focused on the development and optimization of RO-based water treatment systems. V. N. Epimakhov [9] discussed the use of RO filtration in water treatment, while V. V. Goncharuk et al. [10,11] concentrated on the design and implementation of low-pressure RO systems. These efforts have collectively advanced our understanding of RO and its applications in water treatment and desalination. For a more comprehensive review of the literature on RO, readers are referred to [12–14], which provide a wealth of information on the latest developments and findings in this field.

In order to perform the water treatment process in the RO, we must be able to apply pressure to the system and overcome the osmotic pressure. As a result, we will be able to purge the water of pollutants and biological elements like bacteria [15]. The outcome is that the trash must stay in the pressured space while the pure water is moved to the other side. As a result, bigger molecules, such as ions, cannot pass through the membrane, and only tiny molecules can pass through [16]. Due to the model's significance, several researchers have recently investigated the RO model and used it to apply various controls. The model predictive control and dynamic matrix control were combined in [17], and the model predictive control methods were directly examined in [18]. Figure 1 shows the RO system.

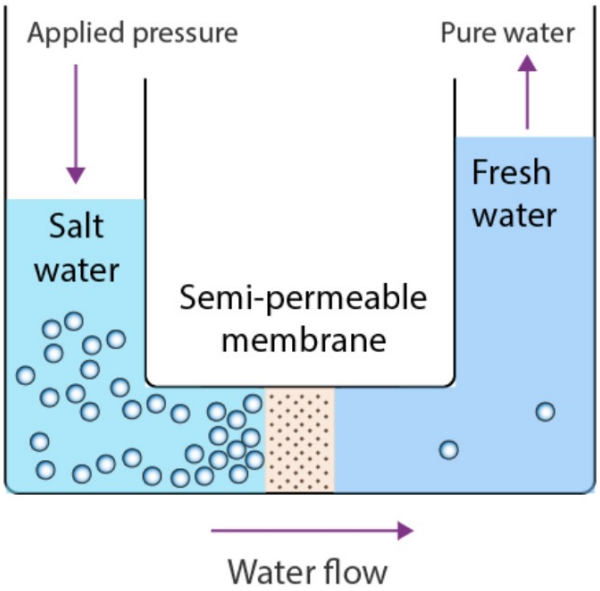


Figure 1. Reverse osmosis system.

Several researchers are investigating the model of the RO system. Luo et al. utilized machine learning techniques to develop an optimal design for the RO system in [19]. Razeghi et al. concentrated on the capability of geographic information systems (GISs) to provide energy to RO devices in [20]. Sayyad et al. [21] designed a hybrid forward system for RO. Kahrizi et al. [22] used computational fluid dynamics modeling to investigate the

relationship between membrane porosity, tortuosity, and the forward water and reverse salt fluxes in forward osmosis. Additional research on the RO system can be found in [23,24].

To predict the concentration of salt solutions in semi-permeable membranes within the RO model, it can be expressed as an advection–diffusion equation [25]:

$$\eta \frac{\partial Q}{\partial z} = \alpha \frac{\partial^2 Q}{\partial \eta^2}, \tag{1}$$

with $\alpha = \frac{Ph}{v_0}$ and the boundary conditions

$$Q(0, \eta) = L_0, \; Q(z, \infty) = L_1, \tag{2}$$

and

$$-P \frac{\partial Q}{\partial \eta}(z, 0) = qQ(z, 0). \tag{3}$$

In this equation, there are constant parameters representing the velocity of water flow through the semi-permeable membrane q, the dispersion of salt in water P, the distance from the semi-permeable boundary to the center of the canal h, and the horizontal velocity at a distance h from the semi-boundary v_0. The variables z and η denote spatial coordinates, while $Q = Q(z, \eta)$ represents the concentration of salt solutions at the point (z, η). The stationary model for reverse osmosis water purification assumes that the system has reached a steady-state condition, where the concentrations of salt solutions are independent of time and the water before and after the membrane is uniformly fouled and purified, respectively.

In [25], Fulford and Broadbridge found the solution of the RO system (1) as

$$Q(z, 0) = \frac{3^{-\frac{1}{3}} q L_0}{P \mathcal{J}} \left(\frac{Ph}{v_0} \right)^{\frac{1}{3}} z^{\frac{1}{3}} + L_0. \tag{4}$$

This model can also be used to estimate the concentration of salt solutions in the RO system, where $\mathcal{J}$ is defined as an improper integral given by $\mathcal{J} = \int_0^\infty exp(-A^3) AdA$. The integral $\mathcal{J}$ presents a significant challenge, as improper integrals are often difficult to solve using direct methods. Therefore, selecting an accurate and efficient numerical method for finding the solution is essential for this study. Typically, the numerical methods employed to tackle engineering problems rely on floating-point arithmetic (F-PA), which involves a specific value, denoted as ε, to manage step sizes and errors. When we have exact and approximate solutions ($\mathcal{J}$ and $\mathcal{J}_\iota$) or two successive approximations ($\mathcal{J}_\iota$ and $\mathcal{J}_{\iota+1}$), we apply certain conditions, such as

$$|\mathcal{J} - \mathcal{J}_\iota| < \varepsilon, \quad or \quad |\mathcal{J}_{\iota+1} - \mathcal{J}_\iota| < \varepsilon. \tag{5}$$

The motivation behind this study stems from a series of fundamental questions that have driven our research and led to the development of this paper. Specifically, we sought to address the following key inquiries:

1. What constitutes an effective stopping condition when applying numerical methods to solve problems, and why is it essential to implement such a condition?
2. How many iterations are required when employing numerical methods, and what factors influence this number?
3. What strategies can be employed to control the number of iterations in numerical methods, and how can they be optimized?
4. How can we determine the optimal approximation when seeking a numerical solution, and what are the implications of this approximation on the overall accuracy of the results?

5. What is the optimal value for the tolerance parameter ε in condition (5), and how can it be determined?
6. How can we control the accuracy of numerical methods using the absolute error (5) when the exact solution is unknown?
7. What approaches can be used to identify the optimal error in numerical methods, and how can this information be leveraged to improve the overall performance of these methods?

These questions, along with several others, have motivated us to undertake this research and develop innovative solutions to address the challenges associated with numerical methods.

The main idea of this research is to cover the mentioned gaps by using the CESTAC method and the CADNA library. In this method, we apply

$$|\mathcal{J}_\iota - \mathcal{J}_{\iota+1}| = @.0, \tag{6}$$

where the informational zero @.0 indicates the equality of the number of common significant digits between two successive iterations [26–31]. This technique is rooted in stochastic arithmetic, and there are studies focused on dynamically controlling numerical methods. The primary innovation of this approach lies in its ability to determine optimal results, errors, and steps for numerical methods. Recently, this method has been utilized to validate numerical results derived from various techniques for solving a range of problems, including numerical integration rules [32–35], interpolation [36], solving integral equations [37,38], optimizing regularization methods [39] and load leveling issues [40]. Our study offers several novel contributions, including:

1. The identification of the optimal iteration of the Romberg integration rule for the RO system, which has significant implications for the efficient solution of this problem.
2. The determination of the optimal approximation of the problem, which provides a benchmark for evaluating the accuracy of numerical methods.
3. The discovery of the optimal error of the Romberg integration rule for the RO model, which enables the optimization of the numerical method for this specific application.
4. The application of dynamical control (6) to regulate the accuracy and efficiency of the numerical method, ensuring that the results are reliable and computationally efficient.
5. The utilization of the CADNA library to implement the CESTAC method mentioned in Section 3, which enables the automatic control of accuracy and efficiency in numerical computations.
6. The development of a strategy to control the accuracy of numerical methods without requiring knowledge of the exact solution, which is a significant advancement in the field.
7. The elimination of the need to specify an epsilon value to control efficiency, which simplifies the implementation of numerical methods and reduces the risk of user error.

We believe that the research addresses significant gaps in the existing literature and provides innovative solutions to pressing challenges in the field of numerical methods.

2. Romberg Integration Rule

This section focuses on the Romberg integration rule [41]. In this approach, we can find our initial estimates using other conventional methods such as the trapezoidal rule

or Simpson's rule. Here, we apply the trapezoidal rule, beginning the process with $\iota = 2$ nodes. Then, doubling ι and utilizing the formula

$$\mathcal{J}_{k,i} = \frac{4^i \mathcal{J}_{k,i-1} - \mathcal{J}_{k-1,i-1}}{4^i - 1}, \tag{7}$$

we can find the approximations one by one in the following table

$$\begin{array}{cccccc} \mathcal{J}_{1,1} & & & & & \\ \mathcal{J}_{2,1} & \mathcal{J}_{2,2} & & & & \\ \mathcal{J}_{3,1} & \mathcal{J}_{3,2} & \mathcal{J}_{3,3} & & & \\ \mathcal{J}_{4,1} & \mathcal{J}_{4,2} & \mathcal{J}_{4,3} & \mathcal{J}_{4,4} & & \\ \mathcal{J}_{5,1} & \mathcal{J}_{5,2} & \mathcal{J}_{5,3} & \mathcal{J}_{5,4} & \mathcal{J}_{5,5} & \cdots \\ \vdots & \vdots & \vdots & \vdots & \vdots & \vdots \end{array}$$

The error for $\mathcal{J}_1(\ell)$ and the order $2\iota + 2$ can be written as [42]

$$\mathbb{E}_1 F = \mathcal{J}_1(\ell) - \mathcal{J} = \sum_{i=1}^{\iota} \frac{\alpha_{2i} \ell^{2i}}{(2i)!} + \mathcal{O}(\frac{\ell^{2\iota+2}}{(2\iota+2)!}), \tag{8}$$

where $\alpha_{2i} = B_{2i}[F^{(2i-1)}(\vartheta_2) - F^{(2i-1)}(\vartheta_1)]$, with the Bs being the Bernoulli numbers. Also for $\mathcal{J}_2(\ell)$, we obtain

$$\mathbb{E}_2 F = \mathcal{J}_2(\ell) - \mathcal{J} = \sum_{i=2}^{\iota} \frac{\alpha_{2i} \ell^{2i}}{(2i)!} \times \frac{1}{4-1}(\frac{1}{4^{i-1}} - 1) + \mathcal{O}\Big(\frac{\ell^{2\iota+2}}{(2\iota+2)!} \times \frac{1}{4-1}(\frac{1}{4^{\iota}} - 1)\Big), \tag{9}$$

Also, $\mathcal{J}_r(\ell),\ r = 2, ..., n$ can be found as

$$\mathbb{E}_r F = \mathcal{J}_r(\ell) - \mathcal{J} = \sum_{i=r}^{\iota} \frac{\alpha_{2i} \ell^{2i}}{(2i)!} \prod_{j=1}^{r-1} \frac{1}{4^j - 1}(\frac{1}{4^{i-j}} - 1) + \mathcal{O}\Big(\frac{\ell^{2\iota+2}}{(2\iota+2)!} \prod_{j=1}^{r-1} \frac{1}{4^j - 1}(\frac{1}{4^{\iota-j+1}} - 1)\Big). \tag{10}$$

Therefore,

$$\mathbb{E}_\iota F = \mathcal{J}_\iota(\ell) - \mathcal{J} = \frac{(-1)^{\iota-1} \alpha_{2\iota} \ell^{2\iota}}{(2\iota)! 2^{\iota(\iota-1)}} + \mathcal{O}\Big(\frac{\ell^{2\iota+2}}{(2\iota+2)! 2^{\iota(\iota-1)}}\Big) \tag{11}$$

and we can approximate the integral as [41]

$$\mathcal{J}(F) = \int_{\vartheta_1}^{\vartheta_2} F(z)dz = \mathcal{J}_\iota(F) + \mathbb{E}(F), \tag{12}$$

where $\mathcal{J}_\iota(F) = h \sum_{i=1}^{\iota} w_i F(z_i)$.

If the initial values of the Romberg integration rule are given by the trapezoidal approximation $\mathcal{J}_{k,1}(F)$ and we denote by $\ell_k = \frac{\vartheta_2 - \vartheta_1}{2^{k-1}}$, then we obtain

$$\begin{aligned}
\mathcal{J}_{1,1}(F) &= \frac{\ell_1}{2}[F(z_0) + F(z_\iota)\Big], \\
\mathcal{J}_{2,1}(F) &= \frac{\ell_2}{2}\Big[F(z_0) + 2F(z_0 + \ell_2) + F(z_\iota)\Big] \\
&= \frac{z_\iota - z_0}{4}\Big[F(z_0) + F(z_\iota) + 2F(z_0 + \frac{z_\iota - z_0}{2})\Big] \\
&= \frac{1}{2}\Big[\mathcal{J}_{1,1}(F) + \ell_1 F(z_0 + \ell_2)\Big]
\end{aligned} \tag{13}$$

and the general relation can be obtained as

$$\mathcal{J}_{k,1}(F) = \frac{1}{2}\Big[\mathcal{J}_{k-1,1}(F) + \ell_{k-1}\sum_{j=1}^{2^{k-2}} F(z_0 + (2j-1)\ell_k)\Big], \quad k = 2, 3, ..., n. \tag{14}$$

Finally, we can write

$$\mathcal{J}_{k,i}(F) = \mathcal{J}_{k,i-1}(F) + \frac{\mathcal{J}_{k,i-1}(F) - \mathcal{J}_{k-1,i-1}(F)}{4^{i-1} - 1}. \tag{15}$$

3. Main Idea

In this section, we explore the fundamental concept of the CESTAC method and how it can be integrated with other numerical techniques to achieve optimal results errors, and steps. This concept is fundamentally rooted in stochastic arithmetic. It is important to note that this method is not a problem-solving scheme; rather, it serves as a technique for validating the outcomes of various numerical methods [26–28].

Assume that A is a set of values represented by a computer and G is a member of A that can be written based on computer arithmetic in the form

$$G = g - n_1 2^{z-\rho} n_2, \tag{16}$$

where $g \in \mathbb{R}$, with ρ mantissa bits, n_1 shows the sign, $2^{-\rho}n_2$ is the missing segment of the mantissa, and z is the binary exponent. Also, we should note that the results can be produced by single and double precisions for $\rho = 24, 53$.

By assuming n_2 to be uniformly distributed on $[-1, 1]$, we can apply small perturbations on the last bit of mantissa. Thus, we will be able to have the mean (μ) and the standard deviation (σ) values for the results of G. By repeating the process for m times, we will have a quasi-Gaussian distribution for $G_k, k = 1, ..., m$, which means that we will have equality between the mean value of the sample and G. On the other hand, in order to control the numerical procedure, we can find the number of common significant digits between the mean value G_{ave} and G, using

$$C_{G_{ave},G} = \log_{10} \frac{\sqrt{m}|G_{ave}|}{\tau_\delta \sigma}.$$

Here, τ_δ represents the value from the T distribution, while $1 - \delta$ indicates the confidence interval with $m - 1$ degrees of freedom. The algorithm will terminate and display the informational zero @.0 when $G_{ave} = 0$ or $C_{G_{ave},G} \leq 0$. To apply the CESTAC method,

direct implementation is not necessary. Instead, writing CADNA codes allows the library to implement the method and validate numerical results. These codes can be written in programming languages such as C, C++, FORTRAN, or ADA and executed on the Linux operating system [28–31]. The following algorithm (Algorithm 1) is the general algorithm of the CESTAC method.

Algorithm 1: CESTAC Algorithm

`Step 1--Make the perturbation of the last bit of mantissa to produce` J `samples of` G `as` $\Phi = \{G_1, G_2, ..., G_J\}$.

`Step 2--Find` $G_{ave} = \dfrac{\sum_{i=1}^{J} G_i}{J}$.

`Step 3--Compute` $\sigma^2 = \dfrac{\sum_{i=1}^{J}(G_i - G_{ave})^2}{J-1}$.

`Step 4--Find the NCSDs of` G `and` G_{ave} `applying` $C_{G_{ave},G} = \log_{10} \dfrac{\sqrt{J}|G_{ave}|}{\tau_\delta \sigma}$.

`Step 5--Print` $G =$ `@.0 if` $G_{ave} = 0$, `or` $C_{G_{ave},G} \leq 0$.

The CESTAC method offers several advantages over traditional floating-point arithmetic:

1. The termination criterion is based on two successive approximations, eliminating the need for an exact solution.
2. Unlike floating-point arithmetic, the CESTAC method does not rely on a predefined epsilon value for its stopping condition.
3. The CESTAC method avoids unnecessary iterations, which can occur in floating-point arithmetic when using large epsilon values.
4. It provides the ability to display the number of common significant digits using the informatical zero sign (@.0), a feature not available in floating-point arithmetic.
5. The CESTAC method enables the determination of the optimal approximation, error, and step size for numerical procedures, which is not possible with floating-point arithmetic.
6. Additionally, the CESTAC method can reveal numerical instabilities that may not be apparent in floating-point arithmetic.

Definition 1 ([30,31]). *For $q_1, q_2 \in \mathbb{R}$, the number of common significant digits can be defined as*

$$C_{q_1,q_2} = \log_{10}\left|\frac{q_1+q_2}{2(q_1-q_2)}\right| = \log_{10}\left|\frac{q_1}{q_1-q_2} - \frac{1}{2}\right|, \quad q_1 \neq q_2, \tag{17}$$

and $C_{q_1,q_1} = +\infty$.

Theorem 1. *Let $F(z)$ be a continuous function, $\mathcal{J} = \int_{\vartheta_1}^{\vartheta_2} F(z)dz$, and $\mathcal{J}_\iota$ be an approximation of $\mathcal{J}$, which is obtained by Romberg integration rule. Then,*

$$C_{\mathcal{J}_\iota,\mathcal{J}_{\iota+1}} = C_{\mathcal{J}_\iota,\mathcal{J}} + \mathcal{O}(\frac{\ell^2}{\iota^2}). \tag{18}$$

Proof. Using Definition 1, we obtain

$$C_{\mathcal{J}_\iota,\mathcal{J}} = \log_{10}\left|\frac{\mathcal{J}_\iota + \mathcal{J}}{2(\mathcal{J}_\iota - \mathcal{J})}\right|.$$

Now, we have

$$\frac{\mathcal{J}_\iota + \mathcal{J}}{2(\mathcal{J}_\iota - \mathcal{J})} = \frac{\mathcal{J}_\iota}{\mathcal{J}_\iota - \mathcal{J}} - \frac{1}{2} = \frac{\mathcal{J}_\iota}{\frac{(-1)^{\iota-1}\alpha_{2\iota}\ell^{2\iota}}{(2\iota)!2^{\iota(\iota-1)}} + \mathcal{O}\left(\frac{\ell^{2\iota+2}}{(2\iota+2)!2^{\iota(\iota-1)}}\right)}$$

$$= \frac{\mathcal{J}_\iota}{\frac{(-1)^{\iota-1}\alpha_{2\iota}\ell^{2\iota}}{(2\iota)!2^{\iota(\iota-1)}}\left[1 + \mathcal{O}(\frac{\ell^{2\iota+2}(2\iota)!2^{\iota(\iota-1)}}{(2\iota+2)!2^{\iota(\iota-1)}(-1)^{\iota-1}\alpha_{2\iota}\ell^{2\iota}})\right]}$$

$$= \frac{\mathcal{J}_\iota(2\iota)!2^{\iota(\iota-1)}}{(-1)^{\iota-1}\alpha_{2\iota}\ell^{2\iota}\left[1 + \mathcal{O}(\frac{\ell^2}{(2\iota+2)(2\iota+1)(-1)^{\iota-1}\alpha_{2\iota}})\right]} \tag{19}$$

$$= \frac{\mathcal{J}_\iota(2\iota)!2^{\iota(\iota-1)}}{(-1)^{\iota-1}\alpha_{2\iota}\ell^{2\iota}\left[1 + \mathcal{O}(\frac{\ell^2}{\iota^2})\right]}$$

$$= \frac{\mathcal{J}_\iota(2\iota)!2^{\iota(\iota-1)}}{(-1)^{\iota-1}\alpha_{2\iota}\ell^{2\iota}} \times \left[\frac{1}{1 + \mathcal{O}(\frac{\ell^2}{\iota^2})}\right]$$

$$= \frac{\mathcal{J}_\iota(2\iota)!2^{\iota(\iota-1)}}{(-1)^{\iota-1}\alpha_{2\iota}\ell^{2\iota}} \times \left[1 + \mathcal{O}(\frac{\ell^2}{\iota^2})\right]$$

$$= \frac{\mathcal{J}_\iota(2\iota)!2^{\iota(\iota-1)}}{(-1)^{\iota-1}\alpha_{2\iota}\ell^{2\iota}} + \mathcal{O}\left(\frac{\ell^2(2\iota)!2^{\iota(\iota-1)}}{\iota^2\ell^{2\iota}}\right)$$

$$= \frac{\mathcal{J}_\iota(2\iota)!2^{\iota(\iota-1)}}{(-1)^{\iota-1}\alpha_{2\iota}\ell^{2\iota}} + \mathcal{O}\left(\frac{(2\iota)!2^{\iota(\iota-1)}}{\iota^2\ell^{2\iota-2}}\right).$$

Similarly,

$$\frac{\mathcal{J}_\iota + \mathcal{J}_{\iota+1}}{2(\mathcal{J}_\iota - \mathcal{J}_{\iota+1})} = \frac{\mathcal{J}_\iota(2\iota)!2^{\iota(\iota-1)}}{(-1)^{\iota-1}\alpha_{2\iota}\ell^{2\iota}} + \mathcal{O}\left(\frac{(2\iota)!2^{\iota(\iota-1)}}{\iota^2\ell^{2\iota-2}}\right). \tag{20}$$

From Equations (19) and (20), we deduce

$$C_{\mathcal{J}_\iota,\mathcal{J}_{\iota+1}} = \log_{10}\left|\frac{\mathcal{J}_\iota(2\iota)!2^{\iota(\iota-1)}}{(-1)^{\iota-1}\alpha_{2\iota}\ell^{2\iota}}\right| + \log_{10}\left(1 + \mathcal{O}(\frac{\ell^2}{\iota^2})\right),$$

and finally,

$$C_{\mathcal{J}_\iota,\mathcal{J}_{\iota+1}} = C_{\mathcal{J}_\iota,\mathcal{J}} + \mathcal{O}\left(\frac{\ell^2}{\iota^2}\right). \tag{21}$$

□

4. Numerical Results

In this section, first, we discuss the general CADNA algorithm on the Romberg integration rule to improve the accuracy of the RO model. As we can see, we have covered both the difference between two successive approximations, as well as the absolute error. And when we obtain @.0, the algorithm will stop. Thus, the new algorithm (Algorithm 2) is not dependent on a value like ε.

Algorithm 2: CESTAC Algorithm for the RO system

```
Step 1:  Put ι = 1;
Step 2:  Enter a, b;
Step 3:  Do:
{
  Step 3-1:  Apply Equation (13) to find the initial approximations;

  Step 3-2:  Calculate other approximations using Equation (15);
  Step 3-3:  Print ι, J_ι, |J_{ι+1} − J_ι| and |J − J_ι|;
  Step 3-4:  ι = n + 1;
} while |J_{ι+1} − J_ι| ≠ @.0.
```

By employing the CESTAC method along with the CADNA library, we can derive optimal iterations, approximations, and errors. To evaluate $\mathcal{J}$, we consider the interval $[0, m]$, where m is sufficiently large such that $|\int_m^\infty e^{-v^3} v dv| = @.0$, indicating that this value has no significant digits. By selecting $m = 10$, we obtain:

$$\mathcal{J} = \int_0^{10} e^{-v^3} v dv = 0.4513726464754668\ldots .$$

The results of our numerical experiments are presented in Table 1, which provides a comprehensive summary of the approximate solution, the difference between two successive approximations, and the absolute error. Notably, the absolute error calculation was performed using results from other methods, as the exact solution was not readily available. A closer examination of Table 1 reveals that the optimal step for the Romberg integration is $\iota_{opt} = 16$, yielding an optimal approximation of $\mathcal{J}_{16} = 0.4513726464755$. The appearance of an informational zero indicates that the number of common significant digits between the differences of two successive approximations and the exact and approximate solutions has reached equality, thereby triggering the algorithm to terminate at $\iota = 16$.

Table 1. The results of the Romberg integration rule using the CESTAC method.

ι	$\mathcal{J}_{\iota+1}$	$\lvert\mathcal{J}_{\iota+1} - \mathcal{J}_\iota\rvert$	$\lvert\mathcal{J}_\iota - \mathcal{J}\rvert$
1	$0.304949145163061\times10^{-1}$	$0.304949145163061\times10^{-1}$	0.420877731959160
2	0.594149303635848	0.563654389119542	0.14277665716038
3	−0.200760426946730	0.794909730582579	0.652133073422197
4	0.761872617669618	0.962633044616349	0.310499971194151
5	0.465708721516427	$0.5166096557688\times10^{-2}$	$0.14336075040960\times10^{-1}$
6	0.444491866350899	$0.19175506470476\times10^{-1}$	$0.6880780124567\times10^{-2}$
7	0.45383696884876	$0.3941087914349\times10^{-1}$	$0.2011050409409\times10^{-2}$
8	0.45126413292979	$0.350959223824\times10^{-2}$	$0.10851354567\times10^{-3}$
9	0.451374180171874	$0.11005252904\times10^{-3}3$	0.153369640×10^{-5}
10	0.451372647634939	0.155793983×10^{-5}	0.115947×10^{-8}
11	0.45137264624239	0.13844×10^{-8}	0.23306×10^{-9}
12	0.45137264647676	0.25229×10^{-9}	0.129×10^{-11}
13	0.45137264647560	0.9×10^{-13}	0.13×10^{-12}
14	0.45137264647578	0.28×10^{-12}	0.31×10^{-12}
15	0.45137264647560	0.1×10^{-12}	0.1×10^{-12}
16	0.4513726464755	@.0	@.0

In contrast, Tables 2 and 3 present the results obtained using the SE/DE Sinc integration rules. For single precision, the optimal iteration is found to be 545, whereas for double precision, it is significantly reduced to 78. A comparative analysis of these results with our

own findings reveals that the CESTAC-based Romberg integration rule outperforms the Sinc integration in terms of efficiency.

Table 2. The results of the SE Sinc integration rule applying the CESTAC.

ι	$\mathcal{J}_{\iota+1}$	$\lvert\mathcal{J}_{\iota+1}-\mathcal{J}_{\iota}\rvert$	$\lvert\mathcal{J}_{\iota+1}-\mathcal{J}\rvert$
1	0.84180×10^{-15}	0.84180×10^{-15}	0.451372646475465
2	0.71243×10^{-8}	0.71243×10^{-8}	0.4513726393511
3	0.10741×10^{-4}	0.10734×10^{-4}	0.4513619048
⋮	⋮	⋮	⋮
543	0.451372646475176	0.9×10^{-14}	0.290×10^{-12}
544	0.45137264647518	0.8×10^{-14}	0.28×10^{-12}
545	0.451372646475192	@.0	0.27×10^{-12}

Table 3. The results of the DE Sinc integration rule applying the CESTAC.

N	$\mathcal{J}_{N+1}$	$\lvert\mathcal{J}_{N+1}-\mathcal{J}_{N}\rvert$	$\lvert\mathcal{J}_{N+1}-I\rvert$
1	$-0.74872505235097\times10^{-1}$	$0.74872505235097\times10^{-1}$	0.52624515171056
2	$-0.604727538493393\times10^{-2}$	$0.68825229850163\times10^{-1}$	0.457419921860400
⋮	⋮	⋮	⋮
44	0.451372644708314	0.131409×10^{-8}	0.176715×10^{-8}
45	0.451372645943506	0.123519×10^{-8}	0.531960×10^{-9}
⋮	⋮	⋮	⋮
77	0.451372646475445	0.1×10^{-13}	0.20×10^{-13}
78	0.451372646475444	@.0	0.2×10^{-13}

To further illustrate the relative performance of these methods, Table 4 provides a comprehensive comparison of the number of iterations required for various values between the Romberg integration rule with double precision, the Sinc integration rule with double exponential decay (DE), and single exponential decay (SE). The results, based on floating-point arithmetic and the stopping condition (5), demonstrate that larger values result in fewer iterations, while smaller values lead to more iterations due to the absence of the optimal value. This observation highlights the importance of carefully selecting the value to achieve optimal performance.

Moreover, the data presented in Table 4 underscore the superiority of the CESTAC-based Romberg integration rule, which consistently requires fewer iterations to achieve a specified level of accuracy compared with the Sinc integration rules. This finding has significant implications for the development of efficient numerical integration methods as it suggests that the CESTAC-based approach can provide substantial computational savings without compromising accuracy.

Consequently, the optimal solution for the RO model can be expressed as

$$\frac{Q(z,0)}{L_0} = 1.5361171751\left(\frac{q}{P}\right)\left(\frac{Ph}{A_0}\right)^{\frac{1}{3}} z^{\frac{1}{3}} + 1,$$

which serves as a mathematical formula to predict the concentration of salt solutions in semi-permeable membranes within the RO model.

Table 4. The number of iterations in Romberg and Sinc integrations for different ε.

Method	ε	Small Values	$\varepsilon = 10^{-5}$	$\varepsilon = 10^{-3}$	$\varepsilon = 10^{-1}$	$\varepsilon = 0.5$	Large Values
Romberg Integration	ι	$>> 6$	6	5	3	1	1
DE Sinc Integration	ι	$>> 17$	17	12	8	2	1
SE Sinc Integration	ι	$>> 120$	120	59	18	1	1

5. Conclusions

The RO system is one of the most important and applicable methods for water purification. It can be modeled as a mathematical problem, and by using numerical integration methods, we can find an approximate solution to the model. This will help improve purification processes in both industrial and residential systems. Therefore, it is crucial to identify an accurate and applicable method for solving the model. Some researchers have addressed this model, but their methods were based on floating-point arithmetic. To demonstrate the accuracy of their methods, they applied traditional absolute error, which in some cases depended on a small positive value, ε. In this study, we applied the Romberg integration rule and introduced the CESTAC method to find the approximate solution for the RO system. We utilized the CADNA library to implement the CESTAC method, which is designed to run on a Linux operating system. This approach allows us to determine the optimal approximation, optimal error, and optimal iteration of the numerical procedure. We compared the number of iterations based on F-PA for different values of ε. The results indicate that Romberg integration is faster and more accurate than the previously mentioned methods. For future studies, we propose exploring the fuzzy form of this problem, which includes designing the system, finding solutions, and solving the fuzzy integral using novel methods.

Author Contributions: Methodology, S.N. and S.M.; software, S.N.; validation, S.N. and S.M.; formal analysis, S.N.; investigation, S.N. and S.M.; writing—original draft, S.N.; writing—review and editing, S.N. and S.M. All authors have read and agreed to the published version of the manuscript.

Funding: The work of S. Noeiaghdam was funded by the High-Level Talent Research Start-up Project Funding of Henan Academy of Sciences (Project No. 241819246).

Data Availability Statement: The original contributions presented in this study are included in the article. Further inquiries can be directed to the corresponding author.

Conflicts of Interest: The authors declare no conflicts of interest.

Abbreviations

The following abbreviations are used in this manuscript:

RO	Reverse osmosis
CESTAC	Controle et Estimation Stochastique des Arrondis de Calculs
CADNA	Control of Accuracy and Debugging for Numerical Applications
F-PA	Floating-point arithmetic

References

1. Hui, J.; Ling, J.; Dong, H.; Wang, G.; Yuan, J. Distributed parameter modeling for the steam generator in the nuclear power plant. *Ann. Nucl. Energy* **2021**, *152*, 107945. [CrossRef]
2. Garud, R.M.; Kore, S.V.; Kore, V.S.; Kulkarni, G.S. A short review on process and applications of reverse osmosis. *Univers. J. Environ. Res. Technol.* **2011**, *1*, 233–238.

3. Hosseinzadeh, A.; Altaee, A.; Ibra, I.; Zhou, J.L. Modeling and optimization of reverse salt diffusion and water flux in forward osmosis by response surface methodology and artificial neural network. *Chem. Eng. Process.-Process. Intensif.* **2025** , *208*, 110140. [CrossRef]
4. Wang, X.; Sun, X.; Wu, Y.; Gao, F.; Yang, Y. Optimizing reverse osmosis desalination from brackish waters: Predictive approach employing response surface methodology and artificial neural network models. *J. Membr. Sci.* **2024**, *704*, 122883. [CrossRef]
5. Fan, H.; Heiranian, M.; Elimelech, M. The solution-diffusion model for water transport in reverse osmosis: What went wrong? *Desalination* **2024**, *580*, 117575. [CrossRef]
6. Zhai, Y.; Liu, G.; van der Meer, W.G.J. One-Step Reverse Osmosis Based on Riverbank Filtration for Future Drinking Water Purification. *Engineering* **2022**, *9*, 27–34. [CrossRef]
7. Zhang, B.; Jiang, Y.; Fang, F.; Zhang, K. Membrane fouling in reverse-osmosis filters during real drinking water purification: Impact of operation modes and pretreatment. *Desalin. Water Treat.* **2019**, *159*, 214–223 [CrossRef]
8. Jamil, S.; Jeong, S.; Vigneswaran, S. Application of pressure assisted forward osmosis for water purification and reuse of reverse osmosis concentrate from a water reclamation plant. *Sep. Purif. Technol.* **2016**, *171*, 182–190. [CrossRef]
9. Epimakhov, V.N.; Oleinik, M.S. Reverse-Osmosis Filtration Based Water Treatment and Special Water Purification for Nuclear Power Systems. *At. Energy* **2004**, *96*, 234–240. [CrossRef]
10. Goncharuk, V.V.; Osipenko, V.O.; Balakina, M.N. Water purification of nitrates by low-pressure reverse osmosis method. *J. Water Chem. Technol.* **2013**, *35*, 71–75. [CrossRef]
11. Goncharuk, V.V.; Deremeshko, L.A.; Balakina, M.N. Purification of waters containing fluorine by low pressure reverse osmosis for their complex treatment. *J. Water Chem. Technol.* **2013**, *35*, 122–127. [CrossRef]
12. Ma, S.; Wu, X.; Fan, L.; Xie, Z. Predicting water flux and reverse solute flux in forward osmosis processes using artificial neural networks (ANN) modelling with structural parameters. *Sep. Purif. Technol.* **2024**, *351*, 128092. [CrossRef]
13. Afarinandeh, A.; Rashidi, H.; Karimi, L.; Heidari, K.; Arashi, A. Box–Behnken multi-response modeling and optimizing of brackish water reverse osmosis brine treatment using electrodialysis reversal with tortuous flow path. *Desalin. Water Treat.* **2023**, *303*, 11–23. [CrossRef]
14. Teng, Y.; Ng, H.Y. Prediction of reverse osmosis membrane fouling in water reuse by integrated adsorption and data-driven models. *Desalination* **2024**, *576*, 117353. [CrossRef]
15. Wimalawansa, S.J. Purification of contaminated water with reverse osmosis: Effective solution of providing clean water for human needs in developing countries. *Int. J. Emerg. Technol. Adv. Eng.* **2013**, *3*, 75–89.
16. Warsinger, D.M.; Tow, E.W.; Nayar, K.G.; Maswadeh, L.A.; Lienhard, V.J.H. Energy efficiency of batch and semi-batch (CCRO) reverse osmosis desalination. *Water Res.* **2016**, *106*, 272–282. [CrossRef] [PubMed]
17. Paulina Maure, O.; Mungkasi, S. Application of numerical integration in solving a reverse osmosis model. *AIP Conf. Proc.* **2019**, *2202*, 020043.
18. Bartman, A.R.; McFall, C.W.; Christofides, P.D.; Cohen, Y. Model-predictive control of feed flow reversal in a reverse osmosis desalination process. *J. Process. Control.* **2009**, *19*, 433–442. [CrossRef]
19. Luo, J.; Li, M.; Hoek, E.M.V.; Heng, Y. Supercomputing and machine learning-aided optimal design of high permeability seawater reverse osmosis membrane systems. *Sci. Bull.* **2023**, *68*, 397–407. [CrossRef]
20. Razeghi, M.; Hajinezhad, A.; Naseri, A.; Noorollahi, Y.; Moosavian, S.F. Multi-criteria decision for selecting a wind farm location to supply energy to reverse osmosis devices and produce freshwater using GIS in Iran. *Energy Strategy Rev.* **2023**, *45*, 101018. [CrossRef]
21. Sayyad, S.U.; Kamthe, N.K.; Sarvade, S.M. Design and simulation of reverse osmosis process in a hybrid forward osmosis-reverse osmosis system. *Chem. Eng. Res. Des.* **2022**, *183*, 210–220. [CrossRef]
22. Kahrizi, M.; Lin, J.; Ji, G.; Kong, L.; Song, C.; Dumée, L.F.; Sahebi, S.; Zhao, S. Relating forward water and reverse salt fluxes to membrane porosity and tortuosity in forward osmosis: CFD modelling. *Sep. Purif. Technol.* **2020**, *241*, 116727. [CrossRef]
23. Yang, Y.; Wang, Z.; Song, Z.; Liu, D.; Zhang, J.; Guo, L.; Fang, W.; Jin, J. Thermal treated amidoxime modified polymer of intrinsic microporosity (AOPIM-1) membranes for high permselectivity reverse osmosis desalination. *Desalination* **2023**, *551*, 116413. [CrossRef]
24. Singh, C.P.; Patel, R.V.; Yadav, A.; Kumar, A. Numerical simulations of the effect on twisted spacer filaments on biofouling and scaling in the feed channel of reverse osmosis membrane modules. *Colloids Surfaces Physicochem. Eng. Asp.* **2023**, *666*, 131333. [CrossRef]
25. Fulford, G.R.; Broadbridge, P. *Industrial Mathematics: Case Studies in the Diffusion of Heat and Matter*; Cambridge University Press: Cambridge, UK, 2002.
26. Alt, R.; Lamotte, J.-L.; Markov, S. Stochastic arithmetic Theory and experiments. *Serdica J. Comput.* **2010**, *4*, 1–10. [CrossRef]
27. Scott, N.S.; Jézéquel, F.; Denis, C.; Chesneaux, J.-M. Numerical 'health check' for scientific codes: The CADNA approach. *Comput. Phys. Comm.* **2007**, *176*, 507–521. [CrossRef]
28. Graillat, S.; Jézéquel, F.; Wang, S.; Zhu, Y. Stochastic arithmetic in multi precision. *Math. Comput. Sci.* 2011, 5, 359–375. [CrossRef]

29. Graillat, S.; Jézxexquel, F.; Picot, R. Numerical Validation of Compensated Summation Algorithms with Stochastic Arithmetic. *Electron. Notes Theor. Comput. Sci.* **2015**, *317*, 55–69. [CrossRef]
30. Vignes, J. Discrete Stochastic Arithmetic for Validating Results of Numerical Software. *Numer. Algorithms* **2004**, *37*, 377–390. [CrossRef]
31. Vignes, J. A stochastic arithmetic for reliable scientific computation. *Math. Comput. Simul.* **1993**, *35*, 233–261. [CrossRef]
32. Abbasbandy, S.; Araghi, M.A.F. Numerical solution of improper integrals with valid implementation. *Math. Comput. Appl.* **2002**, *7*, 83–91. [CrossRef]
33. Abbasbandy, S.; Araghi, M.A.F. The valid implementation of numerical integration methods. *Far East J. Appl. Math.* **2002**, *8*, 89–101.
34. Abbasbandy, S.; Araghi, M.A.F. A stochastic scheme for solving definite integrals. *Appl. Numer. Math.* **2005**, *55*, 125–136. [CrossRef]
35. Araghi, M.A.F.; Noeiaghdam, S. Dynamical control of computations using the Gauss-Laguerre integration rule by applying the CADNA library. *Adv. Appl. Math. Sci.* **2016**, *16*, 1–18.
36. Abbasbandy, S.; Araghi, M.A.F. The use of the stochastic rithmetic to estimate the value of interpolation polynomial with optimal degree. *Appl. Numer. Math.* **2004**, *50*, 279–290. [CrossRef]
37. Noeiaghdam, S.; Araghi, M.A.F. Valid implementation of the Sinc-collocation method to solve the linear integral equations by CADNA library. *J. Math. Model.* **2019**, *7*, 63–84.
38. Noeiaghdam, S.; Araghi, M.A.F.; Abbasbandy, S. Finding optimal convergence control parameter in the homotopy analysis method to solve integral equations based on the stochastic arithmetic. *Numer. Algorithms* **2019**, *81*, 237–267. [CrossRef]
39. Noeiaghdam, S.; Araghi, M.A.F. A novel approach to find optimal parameter in the homotopy-regularization method for solving integral equations. *Appl. Math. Inf. Sci.* **2020**, *14*, 105–113.
40. Noeiaghdam, S.; Sidorov, D.; Muftahov, I.; Zhukov, A.V. Control of Accuracy on Taylor-Collocation Method for Load Leveling Problem. *Bull. Irkutsk. State Univ. Ser. Math.* **2019**, *30*, 59–72. [CrossRef]
41. Iyengar, S.R.K.; Jain, R.K. *Numerical Methods*; New Age International Publisher: New Delhi, India, 2020.
42. Atkinson, K.E. *An Introduction to Numerical Analysis*, 2nd ed.; John Wiley: Hoboken, NJ, USA, 1991.

Disclaimer/Publisher's Note: The statements, opinions and data contained in all publications are solely those of the individual author(s) and contributor(s) and not of MDPI and/or the editor(s). MDPI and/or the editor(s) disclaim responsibility for any injury to people or property resulting from any ideas, methods, instructions or products referred to in the content.